Int. J. Multiphase Flow Vol. 18, No. 5, pp. 765–777, 1992
Printed in Great Britain.

0301-9322/92 $5.00 + 0.00

NON-NEWTONIAN EFFECTS ON THE DRAG OF CREEPING FLOW THROUGH PACKED BEDS

J. ZHU and M. G. SATISH
Department of Civil Engineering, Technical University of Nova Scotia, Halifax, Nova Scotia, Canada B3J 2X4

(Received 25 April 1991; in revised form 14 May 1992)

Abstract—Slow flows of non-Newtonian fluids through packed beds of solid particles are studied numerically and analytically using the free-surface cell model to account for the interactions between particles. The flow problem of a Carreau fluid is solved by the finite difference method and that of a second-order fluid by the perturbation method. It is shown that the flow drag decreases with a decrease in the flow behavior index and with an increase in the characteristic time. The degree of this reduction is found to be more significant at low voidages. The numerical results are found to be closer to the lower bounds obtained using variational principles by earlier investigators. The perturbation solutions predict that the second normal stress difference coefficient has a significant influence on the flow resistance. The flow resistance can either increase or decrease with an increase in the Deborah number, according to the values of the second normal stress difference coefficient. The results are found to be in agreement with the experimental findings that the viscoelastic flow through packed beds can exhibit a rapid increase in the flow resistance, over and above that expected for a comparable viscous fluid, in the second normal stress difference coefficient range for most real viscoelastic fluids.

Key Words: flow drag, non-Newtonian fluid, cell model, packed beds, pseudoplasticity, viscoelasticity

1. INTRODUCTION

The wide occurrence of non-Newtonian fluids has motivated the investigation of the flow behavior of these fluids in multi-particle systems. Examples of such flow include movement of aqueous solutions of polymers through sand and sandstone in tertiary oil recovery operations, the filtration of polymer solutions and slurries and the flow of polymer solutions and melts through granular beds in catalytic polymerization in hydroxydation processes. Experimental evidence indicates that the flow of viscoelastic fluids through packed beds can exhibit a rapid increase in the pressure drop over and above that expected for a comparable viscous fluid (Marshall & Metzner 1976; James & MacLaren 1975; Durst & Haas 1981).

The capillary model was originally used by Christopher & Middleman (1965) to develop a modified Blake–Kozeny equation. This modified Blake–Kozeny equation was used to correlate experimental data on the pressure drop for non-Newtonian fluid flow in fixed and fluidized beds by a number of investigators (Kemblowski & Michniewicz 1979; Kemblowski & Dzuibinski 1978; Brea *et al.* 1986; Mishra *et al.* 1975; Park *et al.* 1975; Kemblowski & Mertl 1974; Siskovic *et al.* 1971; Yu *et al.* 1968; Gregory & Griskey 1967; Gaitonde & Middleman 1967). It should be noted that the capillary model neglects the elongational flows in the real packed beds, which are significantly important for the flow resistance of viscoelastic fluids. Because of this, conflicting conclusions have been reached by different investigators in simulating the viscoelastic flow through packed beds.

The second approach to modeling flow through multi-particle systems is the cell model. According to this model, each particle, assumed uniformly spaced in the assemblage, is enveloped by a spherical fluid cell which represents the interactions between the particles. The radius of this hypothetical surface is related to the voidage of the assemblage considered. In the free-surface cell model of Happel (1958), the shear stress vanishes on the cell surface. It has been indicated that the cell model is an excellent alternative approach to the capillary model in analyzing the creeping flow of non-Newtonian fluids in multi-particle systems (Happel & Brenner 1973; El-Kaissy & Homsy 1973).

A few theoretical studies have been carried out on the flow of non-Newtonian fluids through multi-particle systems. The free-surface cell model has been extended to power law fluids and to the Ellis fluid model by Mohan & Raghuraman (1976a, b) and to the Carreau fluid model by Chhabra & Raghuraman (1984). They obtained upper and lower bounds on the drag coefficient for an assemblage of solid spheres by using a combination of Happel's free-surface cell model and the variational principles. It should be pointed out that the variational results are sensitive to the choice of the trial functions used in the analysis and it is not possible to estimate *a priori* the error inherent in the predicted bounds. Kawase & Ulbrecht (1981) have obtained an approximate solution to the equations of motion for power law flow through an assemblage of solid spheres under the assumption that the deviation from the Newtonian flow behavior was slight. Satish & Zhu (1992) have calculated numerically the flow drag and the mass transfer rate for a power law fluid in multi-particle systems. Although the power law model provides the simplest representation of the shear thinning behavior of non-Newtonian fluids, it cannot predict a constant viscosity in the limit of small shear rates. The Carreau model is superior to the power law model and has been found to be a useful model in representing the shear thinning behavior of non-Newtonian fluids. There is very little theoretical work, as far as we know, relating the viscoelastic flow through multi-particle systems, and there is no general consensus with regard to the influence of the fluid elasticity on the flow in multi-particle systems. Zhu (1990) has obtained an approximate solution for the flow of a third-order fluid through packed beds in some special cases and reported a significant influence of the fluid elasticity on the flow resistance.

In this paper, the effects of non-Newtonian flow behavior including the shear thinning and viscoelastic flow behaviors, on the drag of the flow through packed beds at low Reynolds number are discussed. The paper consists of two parts. The first part is aimed at accounting for the effects of shear thinning behavior on the flow drag, while the second part deals with the viscoelastic effects. In the first part, the equations of motion for the Carreau fluids are solved using the finite difference method by applying Happel's free-surface cell model. The numerical results cover a wide range of pseudoplastic anomaly and bed voidages. In the second part, the perturbation solutions for the flow resistance of a viscoelastic fluid through an assemblage of spheres, considering the elastic effects on the flow resistance, are presented by using a second-order fluid model as a first-order elasticity approximation.

2. PSEUDOPLASTIC EFFECTS ON THE FLOW DRAG

2.1. Statement of the Problem

The Carreau fluid model is written as

$$\boldsymbol{\tau}^* = [\eta_\infty + (\eta_0 - \eta_\infty)(1 + 2\Lambda^2\Pi^*)^{(n-1)/2}]\mathbf{D}^* \qquad [1]$$

where $\boldsymbol{\tau}^*$ is the deviatoric stress tensor, $\mathbf{D}^*$ is the rate of deformation tensor, Π^* is the second invariant of $\mathbf{D}^*$, η_0 and η_∞ are two limiting viscosities, n is the flow behavior index and Λ is a characteristic time of the fluids.

Introducing the following variables:

$$\mathbf{D} = \frac{\mathbf{D}^*}{\left(\dfrac{V_0}{R}\right)}, \quad \Pi = \frac{\Pi^*}{\left(\dfrac{V_0}{R}\right)^2}, \quad \lambda = \frac{\Lambda^*}{\left(\dfrac{R}{V_0}\right)}, \quad \tau = \frac{\tau^*}{\eta_0\left(\dfrac{V_0}{R}\right)}, \quad p = \frac{p^* - p_0^*}{\eta_0\left(\dfrac{V_0}{R}\right)},$$

$$\mathbf{v} = \frac{\mathbf{v}^*}{V_0}, \quad \xi = \frac{r}{R}, \quad \psi = \frac{\psi^*}{V_0 R^2}, \qquad [2]$$

where V_0 is the superficial velocity, R is the radius of the spherical particle, λ is a dimensionless characteristic time, p is dimensionless pressure, $\mathbf{v}$ (dimensionless) and $\mathbf{v}^*$ are velocity vectors, ξ is dimensionless radius and the stream function ψ is defined such that

$$v_{(\xi)} = -\frac{1}{\xi^2 \sin\theta}\frac{\partial\psi}{\partial\theta}, \quad v_{(\theta)} = \frac{1}{\xi \sin\theta}\frac{\partial\psi}{\partial\xi}, \qquad [3]$$

one may obtain the equations of motion for steady, incompressible, axisymmetric flow as follows:

$$E^2\psi = \omega\xi \sin\theta \qquad [4]$$

$$[\alpha + (1-\alpha)(1+2\lambda^2\Pi)^{(n-1)/2}]E^2(\omega\xi \sin\theta) + (n-1)(1-\alpha)\lambda^2(1+2\lambda^2\Pi)^{(n-3)/2} \times \left[\frac{\partial \Pi}{\partial \xi}\frac{\partial}{\partial \xi}(\omega\xi \sin\theta) + \frac{\partial \Pi}{\partial \theta}\frac{1}{\xi^2}\frac{\partial}{\partial \theta}(\omega\xi\sin\theta)\right] = 2(1-n)(1-\alpha)\lambda^2 F(\xi,\theta)\sin\theta, \quad [5]$$

where

$$E^2 = \frac{\partial^2}{\partial \xi^2} + \frac{\sin\theta}{\xi^2}\frac{\partial}{\partial\theta}\left(\frac{1}{\sin\theta}\frac{\partial}{\partial\theta}\right), \quad [6]$$

$$F(\xi,\theta) = \frac{\partial}{\partial\xi}\left[(1+2\lambda^2\Pi)^{(n-3)/2}\left(\xi D_{(\xi\theta)}\frac{\partial\Pi}{\partial\xi} + D_{(\theta\theta)}\frac{\partial\Pi}{\partial\theta}\right)\right] - \frac{\partial}{\partial\theta}\left[(1+2\lambda^2\Pi)^{(n-3)/2}\left(D_{(\xi\xi)}\frac{\partial\Pi}{\partial\xi} + \frac{D(\xi\theta)}{\xi}\frac{\partial\Pi}{\partial\theta}\right)\right] \quad [7]$$

and

$$\alpha = \frac{\eta_\infty}{\eta_0}. \quad [8]$$

The boundary conditions are specified on the solid sphere surface as

$$v_{(\xi)}(1,\theta) = v_{(\theta)}(1,\theta) = 0, \quad [9]$$

and on the outer sphere surface as

$$v_{(\xi)}(s,\theta) = \cos\theta, \quad D_{(\xi\theta)}(s,\theta) = 0, \quad [10]$$

where s is the dimensionless radius of the cell related to the voidage of the packed bed by the expression

$$s = \frac{R_1}{R} = (1-\epsilon)^{-1/3}, \quad [11]$$

where R_1 is the radius of the hypothetical fluid envelope and ϵ is the bed voidage. The condition expressed by [10] indicates that the hypothetical spherical surface is frictionless.

2.2. Numerical Solutions

The stream function and vorticity (ω) vary most rapidly near the surface of the sphere, thus requiring a small step size. Far from the surface, a larger step size is adequate. This is achieved by using equal intervals in z ($\xi = e^z$). To obtain numerical solutions for the problem, finite differences are used. The solution consists of the stream function and vorticity fields. The resulting finite difference equations using central space differences are solved using the successive over-relaxation method.

The mesh sizes are varied, depending upon the voidage of the packed beds. A grid of (41×51) was found to simulate accurately the flow resistance for the case of $\epsilon = 0.5$. For instance, when $\epsilon = 0.5$, $n = 0.7$, $\lambda = 1.0$ and $\alpha = 0.0$, drag coefficients of 15.8697 and 15.8563 are obtained with (41×51) and (81×101) meshes, respectively. In order to verify the validity of the present numerical schemes, the numerical results are compared with the analytical solutions of their Newtonian flow counterpart for all the voidages considered. It was found that the stream function is in agreement with the analytical solutions within 0.01%, the vorticity within 0.1% and the drag coefficient was satisfied within 1–2%.

2.3. Flow Drag Calculation

The flow drag on the solid sphere is given as

$$F_D = 2\pi R^2\left[\int_0^\pi (-p^*)_{r=R}\cos\theta\sin\theta\, d\theta - \int_0^\pi (\tau^*_{(r\theta)})_{r=R}\sin^2\theta\, d\theta\right]. \quad [12]$$

The drag coefficient for the non-Newtonian fluid behavior is, therefore

$$Y_D = \frac{C_D}{\left(\frac{24}{\mathrm{Re}}\right)} = -\frac{1}{3}\left[\int_0^\pi p_s(\theta)\cos\theta\sin\theta\, d\theta + \int_0^\pi (\tau_{(\xi\theta)})_{z=0}\sin^2\theta\, d\theta\right], \quad [13]$$

where the surface pressure $p_s(\theta)$ is calculated using the following relation:

$$p_s(\theta) = 2\int_0^{\ln S}\left\{[\alpha + (1-\alpha)(1+2\lambda^2\Pi)^{(n-1)/2}]\frac{\partial\omega}{\partial\theta} - (n-1)(1-\alpha)\lambda^2(1+2\lambda^2\Pi)^{(n-3)/2}D_{(\xi\xi)}\frac{\partial\Pi}{\partial z}\right\}_{\theta=0}\mathrm{d}z + \int_0^{\theta}\left\{[\alpha+(1-\alpha)(1+2\lambda^2\Pi)^{(n-1)/2}]\left(\frac{\partial\omega}{\partial z}+\omega\right) + \omega(n-1)(1-\alpha)\lambda^2(1+2\lambda^2\Pi)^{(n-3)/2}\frac{\partial\Pi}{\partial z}\right\}_{z=0}\mathrm{d}\theta; \quad [14]$$

Re is the Reynolds number defined on the viscosity at zero shear rate,

$$\mathrm{Re} = \frac{\rho V_0 2R}{\eta_0} \quad [15]$$

where ρ is the density of the fluid.

The results of Y_D have been computed for a wide range of model parameters and bed voidages. The effects of the flow behavior index n on the drag coefficient Y_D is shown in figure 1(a, b) for the free-surface cell model simulation. The variation of $\log(Y_\mathrm{D})$ is almost linear with n. As n decreases, Y_D decreases. The degree of reduction becomes weaker as the voidage becomes larger. The theoretical predictions based on the variational principles presented by Chhabra & Raghuraman (1984) are also plotted in figure 1(a, b). It can be seen that the results of the present numerical analysis are near the lower bound of their predictions. A definite advantage of the present analysis is that it predicts the results in a closed form.

Figure 2 shows Y_D as a function of dimensionless characteristic time λ at different values of n and ϵ in the case of negligible η_∞. It can be seen that Y_D decreases as the ϵ increases and it decreases rapidly as λ increases. It can also be noted that in fluids with high pseudoplastic anomaly, the reduction in Y_D becomes more significant at lower values of λ and the degree of this reduction is more pronounced compared with low pseudoplastic anomaly fluids.

The effect of the limiting viscosity η_∞ (i.e. α) on Y_D is shown in figure 3. η_∞ is usually small compared with η_0. Furthermore, η_∞ is reached at values of shear rate so high that they are unlikely

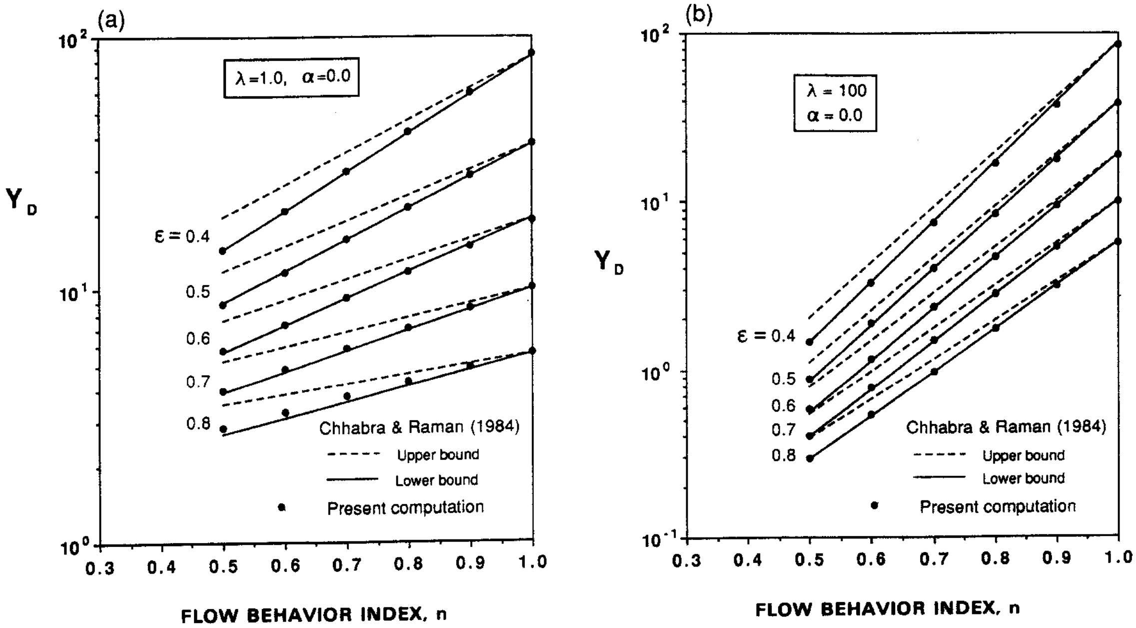

Figure 1. Effect of the flow behavior index n on the drag coefficient Y_D: (a) $\lambda = 1.0$, $\alpha = 0.0$; (b) $\lambda = 100$, $\alpha = 0.0$.

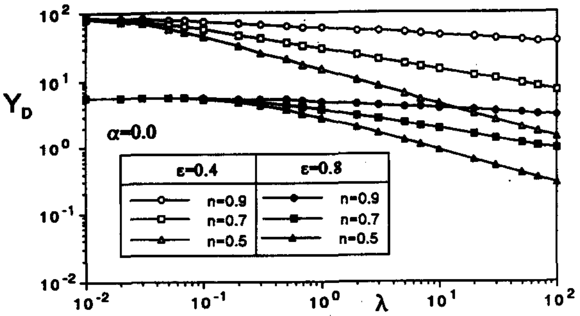

Figure 2. Effect of dimensionless characteristic time λ on the drag coefficient Y_D for $\alpha = 0.0$.

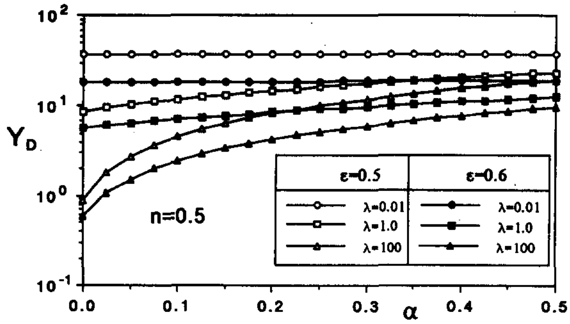

Figure 3. Effect of dimensionless limiting viscosity α on the flow drag Y_D for $n = 0.5$.

to be encountered in creeping flow problems, so the influence of η_∞ (therefore α) is often neglected. Moreover, by inspection of figure 3, one can see that α may have a significant effect on the drag coefficient, especially when λ is high, η_∞ may be reached at lower values of the shear rate if the shear thinning behavior of the fluids is strong, i.e. in the cases of high λ values.

3. VISCOELASTIC EFFECTS ON THE FLOW DRAG

3.1. Perturbation Equations

The constitutive equation of a second-order fluid is written as

$$\boldsymbol{\tau}^* = \eta_0 \overset{(1)}{\mathbf{A}}{}^* + \beta_1 \overset{(1)}{\mathbf{A}}{}^{*2} + \beta_2 \overset{(2)}{\mathbf{A}}{}^*, \qquad [16]$$

where β_1, β_2 are the material constants and $\overset{(n)}{\mathbf{A}}{}^*$ is the nth Rivlin–Ericksen tensor.

The total dimensionless deviatoric stress tensor $\boldsymbol{\tau}$ can be decomposed into two parts.

$$\boldsymbol{\tau} = \overset{(1)}{\mathbf{A}} + \boldsymbol{\tau}^{(e)}, \qquad [17]$$

where $\boldsymbol{\tau}^{(e)} = \sigma(\beta \overset{(1)}{\mathbf{A}}{}^2 + \overset{(2)}{\mathbf{A}})$ is the extra stress caused by non-Newtonian effects and $\sigma = \beta_2 V_0/\eta_0 R$, $\beta = \beta_1/\beta_2$.

The dimensionless equation for the stream function ψ can be written as

$$E^2(E^2\psi) = -\xi \sin\theta[\nabla \times (\nabla \cdot \boldsymbol{\tau}^{(e)})]_{(\phi)}. \qquad [18]$$

Expanding the stream function, velocity, Rivlin–Ericksen tensors and stresses in the form of power series in the perturbation parameter σ, then to the various orders of approximation, one can obtain the following.

Zeroth-order approximations

$$E^2(E^2\psi_0) = 0. \qquad [19]$$

The boundary conditions read

$$v_{(\xi)0}(1,\theta) = v_{(\theta)0}(1,\theta) = 0 \qquad [20]$$

and

$$v_{(\xi)0}(s,\theta) = \cos\theta, \quad \overset{(1)}{\mathbf{A}}_{(\xi\theta)0}(s,\theta) = 0. \qquad [21]$$

Higher-order approximations (i = 1, 2)

$$E^2(E^2\psi_i) = -\xi \sin\theta[\nabla \times (\nabla \cdot \boldsymbol{\tau}_i^{(e)})]_{(\phi)}, \qquad [22]$$

where the higher-order extra-stress $\tau_i^{(e)}$ are

$$\tau_1^{(e)} = \beta \overset{(1)}{\mathbf{A}}{}_0^2 + \overset{(2)}{\mathbf{A}}_0 \quad [23]$$

and

$$\tau_2^{(e)} = \beta(\overset{(1)}{\mathbf{A}}_0 \overset{(1)}{\mathbf{A}}_1 + \overset{(1)}{\mathbf{A}}_1 \overset{(1)}{\mathbf{A}}_0) + \overset{(2)}{\mathbf{A}}_1. \quad [24]$$

The boundary conditions read

$$v_{(\xi)i}(1, \theta) = v_{(\theta)i}(1, \theta) = 0 \quad [25]$$

and

$$v_{(\xi)i}(s, \theta) = 0, \quad \overset{(1)}{A}_{(\xi\theta)i}(s, \theta) = -\tau^{(e)}_{(\xi\theta)i}(s, \theta). \quad [26]$$

3.2. Perturbation Solutions

Zeroth-order solutions

The general solution to [19] is

$$\psi_0 = (a_1 \xi^4 + a_2 \xi^2 + a_3 \xi + a_4 \xi^{-1}) \sin^2 \theta. \quad [27]$$

The constants in [27] should be determined so as to satisfy the boundary conditions [20] and [21], which leads to

$$a_1 = \frac{1}{2(2s^5 - 3s^4 - 2s^{-1} + 3)}, \quad [28a]$$

$$a_2 = -\frac{2s^5 + 3}{2(2s^5 - 3s^4 - 2s^{-1} + 3)}, \quad [28b]$$

$$a_3 = \frac{3s^5 + 2}{2(2s^5 - 3s^4 - 2s^{-1} + 3)}, \quad [28c]$$

and

$$a_4 = -\frac{s^5}{2(2s^5 - 3s^4 - 2s^{-1} + 3)}. \quad [28d]$$

First-order solutions

Assuming that the values of s are $\gg 1$ and neglecting the terms of lower order than ξ^{-4} in deriving an extra-stress tensor $\tau_1^{(e)}$, we have the first-order approximation as follows:

$$E^2(E^2\psi_1) = 12(4\beta + 9)a_3 \xi^{-5} \sin^2 \theta \cos \theta. \quad [29]$$

It may be noted that Kawase & Ulbrecht (1981) have adopted a similar assumption in solving the problem of power law fluids in an assemblage of spherical particles.

The general solution to [29] is

$$\psi_1 = [b_1 \xi^5 + b_2 \xi^3 + b_3 + b_4 \xi^{-2} - \tfrac{1}{2}(4\beta + 9)a_3 \xi^{-1}] \sin^2 \theta \cos \theta. \quad [30]$$

The constants b_1, b_2, b_3, and b_4 in [30] are determined by the boundary conditions:

$$b_1 = \frac{-4(2\beta + 3)(5s^{-9} - 2s^{-6}) - 5(4\beta + 9)s^{-7} + 20(4\beta + 9)s^{-10} - 9(4\beta + 11)s^{-11}}{10(2 - 5s^{-3} + 5s^{-7} - 2s^{-10})} a_3^2, \quad [31a]$$

$$b_2 = \frac{(2 - s - s^{-1})(4b + 9)a_3^2 - 2(2s^6 - 7s + 5s^{-1})b_1}{2(2s^4 - 5s + 3s^{-1})}, \quad [31b]$$

$$b_3 = -\tfrac{1}{2}[7b_1 + 5b_2 - \tfrac{1}{2}(4\beta + 9)a_3^2] \quad [31c]$$

and

$$b_4 = \tfrac{1}{2}[5b_1 + 3b_2 + \tfrac{1}{2}(4\beta + 9)a_3^2]. \quad [31d]$$

Second-order solutions

Neglecting the terms of order lower than ξ^{-4} in deriving the component expressions of the second-order extra-stress tensor $\boldsymbol{\tau}_2^{(e)}$, we have the second-order approximation as follows:

$$E^2(E^2\psi_2) = 12a_3b_3\xi^{-6}\sin^2\theta[28(1+\beta)-(29+32\beta)\sin^2\theta]. \qquad [32]$$

The general solution to [32] is

$$\psi_2 = R_1(\xi)\sin^4\theta + R_2(\xi)\sin^2\theta, \qquad [33]$$

where

$$R_1(\xi) = c_1\xi^6 + c_2\xi^4 + c_3\xi^{-1} + c_4\xi^{-3} + \frac{1}{4}(29+32\beta)a_3b_3\xi^{-2} \qquad [34]$$

and

$$R_2(\xi) = d_1\xi^4 + d_2\xi^2 + d_3\xi + d_4\xi^{-1} - \frac{4}{5}(c_1\xi^6 + c_4\xi^{-3}) - (5+6\beta)a_3b_3\xi^{-2}. \qquad [35]$$

The constants $c_i(1,\ldots,4)$ and $d_j(1,\ldots,4)$ should be determined by the boundary conditions, which leads to:

$$c_1 = \frac{\Delta_1}{\Delta} \qquad [36a]$$

$$c_2 = \frac{\Delta_2}{\Delta} \qquad [36b]$$

$$c_3 = -\frac{1}{8}(29+32\beta)a_3b_3 - \frac{1}{2}(9c_1+7c_2) \qquad [36c]$$

$$c_4 = -\frac{1}{8}(29+32\beta)a_3b_3 + \frac{1}{2}(7c_1+5c_2) \qquad [36d]$$

$$d_1 = \frac{\Sigma_1}{\Sigma} \qquad [37a]$$

$$d_2 = \frac{\Sigma_2}{\Sigma} \qquad [37b]$$

$$d_3 = \frac{1}{2}\left[3(5+6\beta)a_3b_3 + \frac{4}{5}(7c_1-2c_4) - 5d_1 - 3d_2\right] \qquad [37c]$$

$$d_4 = \frac{1}{2}\left[-(5+6\beta)a_3b_3 + \frac{4}{5}(4c_4-5c_1) + 3d_1 + d_2\right]. \qquad [37d]$$

For the expressions of Δ, Δ_1, Δ_2, Σ, Σ_1 and Σ_2, see the Appendix.

3.3. *Viscoelastic Effects on Flow Resistance*

From the force equilibrium on the cell, we obtain the pressure drop over the cell,

$$\frac{\Delta p}{L} = \frac{F_D}{\frac{4}{3}\pi R_1^3} = \frac{3}{2}\frac{\eta_0 V_0}{s^3R^2}(D_0 + D_2\sigma^2), \qquad [38]$$

where

$$D_0 = \frac{2(3s^5+2)}{(2s^5-3s^4-2s^{-1}+3)} \qquad [39]$$

and

$$D_2 = 4d_3 + \frac{2b_3(327+240\beta)(3s^5+2)}{45(2s^5-3s^4-2s^{-1}+3)}. \qquad [40]$$

It is convenient to convert the flow drag to the more familiar quantity $f\mathrm{N_{Re}}$, where the friction factor f and Reynolds number $\mathrm{N_{Re}}$ are defined respectively, as follows:

$$f = \frac{\Delta p}{L}\frac{2R\epsilon^3}{\rho V_0^2(1-\epsilon)} \quad [41]$$

and

$$\mathrm{N_{Re}} = \frac{2R\rho V_0}{\eta_0(1-\epsilon)}. \quad [42]$$

The Deborah number De is defined as

$$\mathrm{De} = \frac{\beta_1 V_0}{\epsilon R\eta_0}. \quad [43]$$

The flow resistance (product of f and $\mathrm{N_{Re}}$) can be written as follows:

$$f\mathrm{N_{Re}} = \mathrm{G}(1 + \mathrm{E\,De}^2), \quad [44]$$

where

$$G = \frac{6D_0\epsilon^3}{(1-\epsilon)} \quad [45]$$

and

$$E = \frac{\epsilon^2 D_2}{4D_0}. \quad [46]$$

Before embarking upon the presentation of the results obtained in this study, it is useful to examine the physical significance of the dimensionless parameter β. From the viscometric calculations, the ratio of the second normal stress difference over the first normal stress difference for a second-order fluid may be obtained as follows:

$$\frac{N_2}{N_1} = -(1 + \tfrac{1}{2}\beta). \quad [47]$$

Results of many viscometric experiments indicate that the second normal stress difference is negative and its absolute value is much smaller than the first normal stress difference, i.e.

$$0 \leqslant (1 + \tfrac{1}{2}\beta) \ll 1. \quad [48]$$

In an earlier study by Zhu (1990), it was assumed that $N_2/N_1 = 0$ in dealing with the third-order fluids of the same flow configuration. A comparison between the results of the present study and those of the earlier study by Zhu (1990) is given in figure 4. The reasonable agreement between these two results indicates that the approximation of neglecting the lower-order terms of ξ in deriving the perturbation equations is acceptible and simplifies greatly the solution procedures.

The effect of viscoelastic flow behavior on the flow drag is shown in figure 5(a, b) in terms of $f\mathrm{N_{Re}}$ and De for four different values of ϵ (0.3, 0.4, 0.7 and 0.99) which cover the condition dealing with strong levels of particle interaction to the flow past a single solid sphere. An inspection of

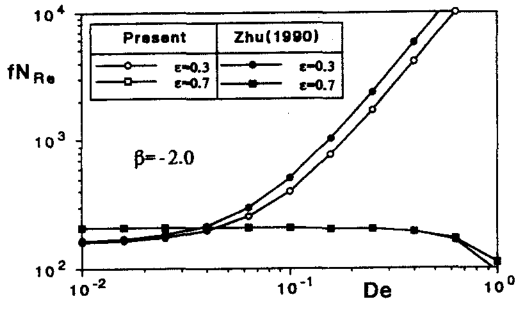

Figure 4. Comparison between the present results and Zhu's (1990) results for $\beta = -2.0$.

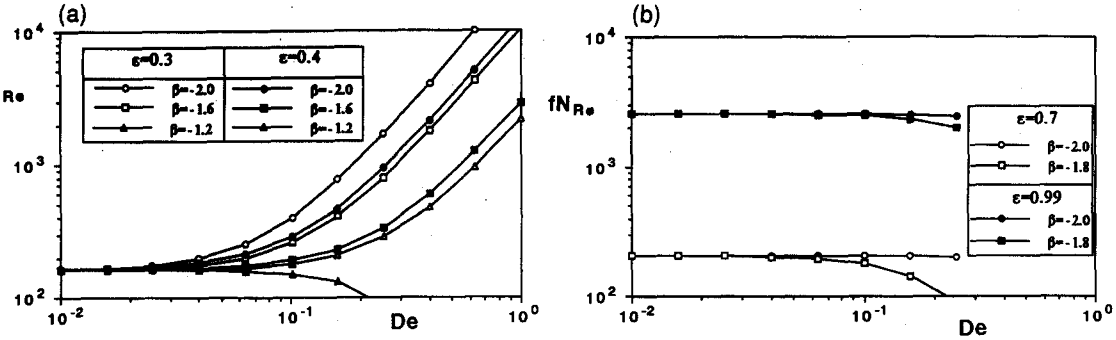

Figure 5. Effect of viscoelastic behavior on the flow resistance $f\mathrm{N_{Re}}$ for different bed voidages ϵ: (a) $\epsilon = 0.3$ and 0.4; (b) $\epsilon = 0.7$ and 0.99.

figure 5(a, b) reveals that both the dimensionless material constant β and the assemblage voidage have a significant influence on the flow resistance. When ϵ is small, the strong particle interaction, which implies strong elongational flow, enhances the flow resistance significantly after De reaches a critical value. The degree of augmentation in $f\mathrm{N_{Re}}$ becomes small as the value of ϵ increases. When ϵ reaches the value of 0.7, $f\mathrm{N_{Re}}$ decreases slightly with the increase in De. For $\epsilon = 0.99$, i.e. in the approximate condition of viscoelastic flow past a single solid sphere, the flow resistance is reduced by fluid elasticity, a result which coincides with the perturbation solutions of Leslie (1961) and Su (1984) for an infinite flow past a single solid sphere.

In figure 6, the dependence of the parameter E in [44] on the dimensionless material constant β is shown. It can be concluded from figure 6 that the influence of the second normal stress difference on the flow resistance is important. The bigger the value of the second normal stress difference coefficient, the smaller will be the influence of the fluid elasticity. For most real viscoelastic fluids, the value of β is around -2.0 and E is generally positive. In the intermediate values of the assemblage voidage ($0.3 \leqslant \epsilon \leqslant 0.6$), viscoelastic flow can exhibit a rapid increase in the pressure, especially for cases with small voidages.

In figure 7, a comparison is made between the present prediction and the experimental data of Marshall & Metzner (1967). In their experiments, a packed bed of particles with a voidage of 0.486 were used. The three kinds of fluids used were a 0.2% aqueous solution of Carbopol 934, 5% PIB L10 in toluene and ET-597 in water, respectively. Viscometric experiments indicate that their relaxation times (extracted from the first normal stress difference measurement) increase successively. In figure 7, Fe and θ_{fl} denote the elasticity factor and the relaxation time of the fluids as shown below, respectively:

$$\mathrm{Fe} = 1 + E\,\mathrm{De}^2 \qquad [49]$$

and

$$\theta_{\mathrm{fl}} = \frac{-\beta_2}{\eta_0}. \qquad [50]$$

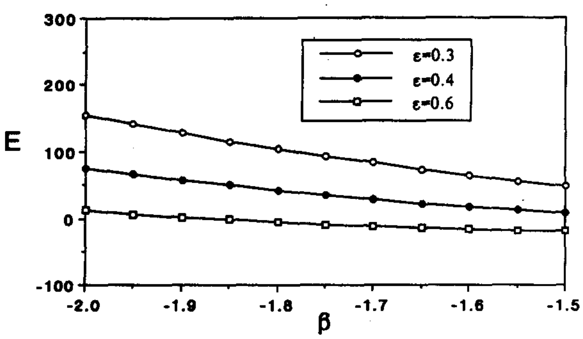

Figure 6. Dependence of the parameter E in [44] on the dimensionless material constant β.

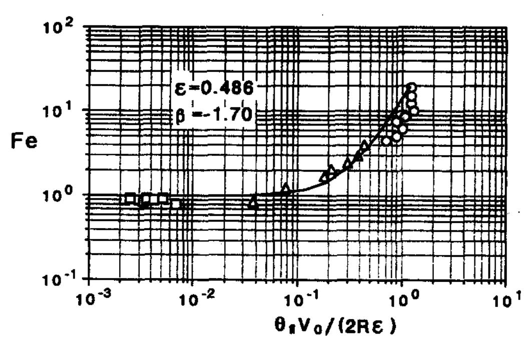

Figure 7. Comparison between the present prediction and Marshall & Metzner's (1967) experimental □, 0.2% Carbopol 934 in water; △, 5% PIB L10 in Decalin; ○, 0.25% ET-597 in water.

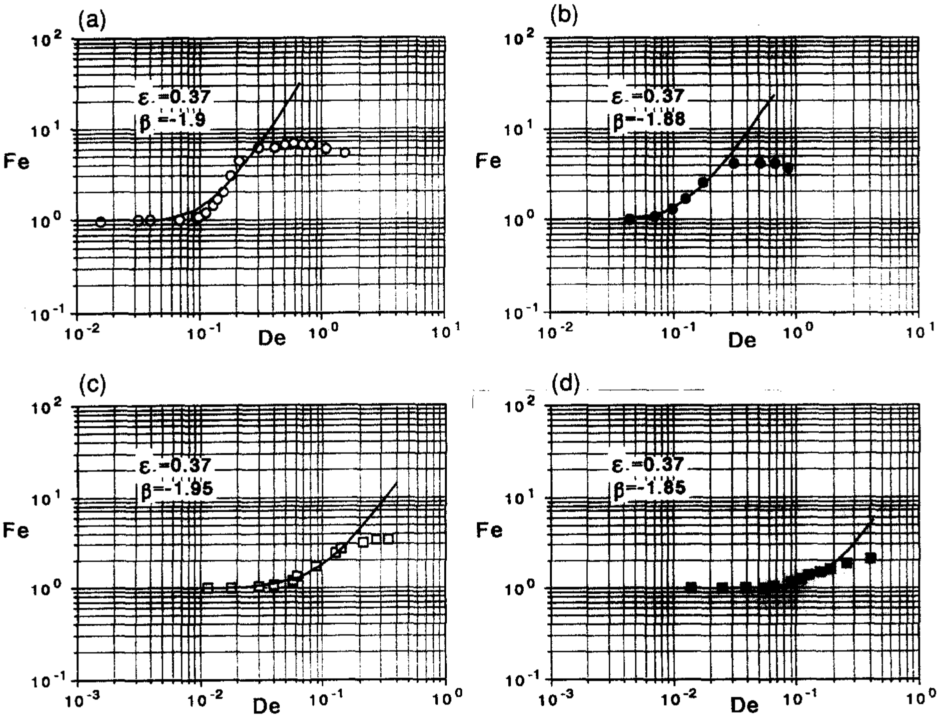

Figure 8. Comparison between the present prediction based on the free-surface cell model and the experimental results of Durst & Haas (1981): (a) PAM W25 in 0.5 M NaCl, $M = 19.23 \times 10^6$, $c = 12.5$ ppm; (b) PAM W968 in 0.5 M NaCl, $M = 10.76 \times 10^6$, $c = 12.5$ ppm; (c) PAM WN23 in 0.5 M NaCl, $M = 3.48 \times 10^6$, $c = 50$ ppm; (d) PAM WN23 in 0.5 M NaCl, $M = 3.48 \times 10^6$, $c = 25$ ppm.

In the present study, for purposes of comparison, we have chosen $\beta = -1.7$, which implies that $N_2/N_1 = -0.15$. It can be seen that the theoretical predictions agree well with the experimental results up to intermediate values of De and overestimate the flow resistances at higher De. The theoretical overestimation at higher De may be due to:

(1) The shear thinning behavior of the real fluids in experiments. Note that the second-order fluid models predict constant viscosity and fail to include the pseudoplasticity of the fluids.

(2) The shortcoming of the second-order fluid model in dealing with the strong elasticity, since the assumption of a second-order fluid is only a weak elasticity approximation of real fluids.

In figure 8(a–d), comparisons between the present predictions and the experimental results of Durst & Haas (1981), using a packed bed of spheres having a voidage of $\epsilon = 0.37$, are shown. It is seen that the present study successfully predicts the flow resistance in low De regions. According to the experimental evidence of Haas & Durst (1982), using simple flow geometries of regularly arranged spheres, the macromolecules of the polymer solutions are stretched step by step and degraded by extension after four contractions. The reduction in flow resistance in high De regions can be explained partly by degradation of the macromolecules under strong extensional flows. It should be noted that both the second-order fluid model and the perturbation method used in the present study are only effective under the assumption of weak elasticity, as mentioned earlier. It has also been observed that (Durst *et al.* 1987; Bird *et al.* 1977), by using the finite extensible non-linear-elastic dumbell model, the elongational viscosity of polymer solutions when exposed to a constant elongational strain rate can be expressed as a polynomial of De only in the asymptotic case of low elongational strain rates. Strong elastic effects on the flow drag in packed beds merit further investigation.

4. CONCLUSIONS

The flow problems of Carreau fluids through packed beds are solved numerically under creeping flow conditions by using the cell model to simplify the multi-particle systems. The drag coefficient has been calculated for the multi-particle systems by finite difference methods. The predicted reduction in the drag coefficient due to the shear thinning behavior of the fluids is found to be closer to the lower bounds of Chhabra & Raghuraman's (1984) findings, obtained by a combination of the free-surface cell model and variational principles. A definite advantage of the present study over Chhabra & Raghuraman's is that it presents the results in a closed form. The results indicate that the degree of drag reduction due to the pseudoplastic behavior is more significant for low voidage beds. It is found that the limiting viscosity η_∞ of fluids has a great influence on the flow drag, although η_∞ is usually small for most shear thinning fluids.

Using a combination of the free-surface cell model for packed beds and the second-order fluid model for fluids, the present study offers a more efficient approximation to the viscoelastic flow through packed beds of solid spheres. The predicted augmentation is in good agreement with the available experimental data up to intermediate values of De. It is found that both the second normal stress difference and the bed voidage have a great influence on the resistance of viscoelastic flow through a packed bed. In cases with small bed voidages, the flow resistance increases with the increase in De in the range of the second normal stress difference for most viscoelastic fluids. In cases with large bed voidages, the flow resistance can decrease with the increase in De. In conclusion, for simulating flow in packed beds, the cell model is more realistic than the classical capillary model since it reflects the elongational flow occurring in real flows through packed beds, which has a significant influence on the flow resistance.

Acknowledgements—The authors are grateful to the referees for their comments which have contributed to the improvement of this paper. Financial support from NSERC Grant No. OGP0036340 is kindly acknowledged.

REFERENCES

Bird, R. B., Hassager, O., Armstrong, R. C. & Curtiss, C. F. 1977 *Dynamics of Polymeric Liquids*; Vol. 2, *Kinetic Theory*. Wiley, New York.

Brea, F. M., Edwards, M. F. & Wilkinson, W. L. 1976 The flow of non-Newtonian slurries through fixed and fluidized beds. *Chem. Engng Sci.* **31**, 329–336.

Chhabra, R. P. & Raghuraman, J. 1984 Slow non-Newtonian flow past an assemblage of rigid spheres. *Chem. Engng Commun.* **27**, 23–46.

Christopher, R. H. & Middleman, S. 1965 Power-law flow through a packed tube. *Ind. Engng Chem. Fundam.* **4**, 422–426.

Durst, F. & Haas, R. 1981 Dehnstromungen mit verdunnten Polymerlosungen: Ein theoretisches Modell und seine experimentelle Verifikation. *Rheol. Acta* **20**, 179–192.

Durst, F., Haas, R. & Interthal, W. 1987 The nature of flows through porous media. *J. Non-Newton. Fluid Mech.* **22**, 169–189.

El-Kaissy, M. M. & Homsy, G. M. 1973 A theoretical study of pressure drop and transport in packed beds at intermediate Reynolds numbers. *Ind. Engng Chem. Fundam.* **12**, 82–90.

Gaitonde, N. Y. & Middleman, S. 1967 Flow of viscoelastic fluids through porous media. *Ind. Engng Chem. Fundam.* **6**, 145–147.

Gregory, D. R. & Griskey, R. G. 1967 Flow of molten polymers through porous media. *AIChE Jl* **13**, 122–125.

Haas, R. & Durst, F. 1982 Viscoelastic flow of dilute polymer solutions in regularly packed beds. *Rheol. Acta* **21**, 566–571.

Happel, J. 1958 Viscous flow in multiparticle systems: slow motion of fluids relative to beds of spherical particles. *AIChE Jl* **4**, 197–201.

Happel, J. & Brenner, H. 1973 *Low Reynolds Number Hydrodynamics*. Noordhoff, Leijden, The Netherlands.

James, D. F. & MacLaren, D. R. 1975 The laminar flow of dilute polymer solutions through porous media. *J. Fluid Mech.* **70**, 733–752.

KAWASE, Y. & ULBRECHT, J. J. 1981 Drag and mass transfer in non-Newtonian flows through multiparticle systems at low Reynolds number. *Chem. Engng Sci.* **36,** 1193–1202.
KEMBLOWSKI, Z. & MERTL, J. 1974 Pressure drop during the flow of Stokesian fluids through granular beds. *Chem. Engng Sci.* **29,** 213–223.
KEMBLOWSKI, Z. & DZUIBINSKI, M. 1978 Resistance to flow of molten polymers through granular beds. *Rheol. Acta* **17,** 176–187.
KEMBLOWSKI, Z. & MICHNIEWICZ, M. 1979 A new look at the laminar flow of power law fluids through granular beds. *Rheol. Acta* **18,** 730–739.
LESLIE, F. M. 1961 The slow flow of a viscoelastic liquid past a sphere. *Q. Jl Mech. Appl Math.* **14,** 36–47.
MARSHALL, R. J. & METZNER, A. B. 1967 Flow of viscoelastic fluids through porous media. *Ind. Engng Chem. Fundam.* **6,** 393–400.
MISHRA, P., SINGH, D. & MISHRA, I. M. 1975 Momentum transfer to Newtonian and non-Newtonian fluids flowing through packed and fluidized beds. *Chem. Engng Sci.* **30,** 397–405.
MOHAN, V. & RAGHURAMAN, J. 1976a A theoretical study of pressure drop for non-Newtonian creeping flow past an assemblage of spheres. *AIChE Jl* **22,** 259–264.
MOHAN, V. & RAGHURAMAN, J. 1976b Bounds on the drag for creeping flow of an Ellis fluid past an assemblage of spheres. *Int. J. Multiphase Flow* **2,** 581–589.
PARK, H. C., HAWLEY, M. C. & BLANKS, R. F. 1975 The flow of non-Newtonian solutions through packed beds. *Polym. Engng Sci.* **15,** 761–773.
SATISH, M. G. & ZHU, 1992 Flow resistance and mass transfer in slow non-Newtonian flow through multiparticle systems. *ASME Jl Appl. Mech.* **59,** 431–437.
SISKOVIC, N., GREGORY, D. R. & GRISKEY, R. G. 1971 Viscoelastic behavior of molten polymers in porous media. *AIChE JL* **17,** 281–285.
SU, Z. D. 1984 The influence of wall on falling sphere in viscoelastic fluids. M.Sc. Thesis, Peking Univ., China.
YU, Y. H., WEN, C. Y. & BAILIE, R. C. 1968 Power law fluids through multiparticle system. *Can. J. Chem. Engng* **46,** 149–154.
ZHU, J. 1990 On the flow resistance of viscoelastic fluids through packed beds. *Rheol. Acta* **29,** 409–415.

APPENDIX

Expressions of Δ, Δ_1, Δ_2, Σ, Σ_1 and Σ_2 in Solutions [36a–d] and [37a–d]

For the requirements of the boundary conditions [25] and [26], we can obtain the linear algebraic equation for the constants c_1, c_2, c_3, c_4, d_1, d_2, d_3 and d_4 as follows:

$$c_1 + c_2 + c_3 + c_4 = \frac{-(29 + 32\beta)a_3 b_3}{4}, \tag{A.1}$$

$$6c_1 + 4c_2 - c_3 - 3c_4 = \frac{(29 + 32\beta)a_3 b_3}{2}, \tag{A.2}$$

$$c_1 s^4 + c_2 s^2 + c_3 s^{-3} + c_4 s^{-5} = \frac{-(29 + 32\beta)a_3 b_3 s^{-4}}{4} \tag{A.3}$$

and

$$15c_1 s^4 + 8c_2 s^2 + 8c_3 s^{-3} + 15c_4 s^{-5} = \frac{-(611 + 376\beta)a_3 b_3 s^{-4}}{4}. \tag{A.4}$$

The solution to the above equations has the form of [36a–d] with the expressions for Δ, Δ_1 and Δ_2 as follows:

$$\Delta = 14(2s^6 - 7s + 7s^{-3} - 2s^{-8}), \tag{A.5}$$

$$\Delta_1 = \frac{[6(35-24\beta)s^{-2} + 7(29+32\beta)s^{-3} - 21(35-24\beta)s^{-7} - 42(29+32\beta)s^{-8} + 20(77+38\beta)s^{-9}]a_3 b_3}{2} \tag{A.6}$$

and

$$\Delta_2 = \frac{[7(29+32\beta)s - 8(77+38\beta) + 27(35-24\beta)s^{-7} + 56(29+32\beta)s^{-8} - 28(77+38\beta)s^{-9}]a_3 b_3}{2}, \quad \text{[A.7]}$$

and

$$d_1 + d_2 + d_3 + d_4 = A_1, \quad \text{[A.8]}$$

$$4d_1 + 2d_2 + d_3 - d_4 = A_2, \quad \text{[A.9]}$$

$$d_1 s^2 + d_2 + d_3 s^{-1} + d_4 s^{-3} = A_3 \quad \text{[A.10]}$$

and

$$d_1 s^2 + d_4 s^{-3} = A_4, \quad \text{[A.11]}$$

where

$$A_1 = 4(c_1 + c_2)/5 + (5 + 6\beta)a_3 b_3, \quad \text{[A.12a]}$$

$$A_2 = 4(6c_1 - 3c_4)/5 + 2(5 + 6\beta)a_3 b_3, \quad \text{[A.12b]}$$

$$A_3 = 4(c_1 s^4 + c_4 s^{-5})/5 + (5 + 6\beta)a_3 b_3 s^{-4}, \quad \text{[A.12c]}$$

$$A_4 = 4c_1 s^4 + 4(c_2 s^2 + c_3 s^{-3})/3 + 4c_4 s^{-5} + (17 + 60\beta)a_3 b_3 s^{-4}/3 \quad \text{[A.12d]}$$

and

$$A_5 = 36c_1 s^4/5 - 4c_2 s^2 + 4c_3 s^{-3} + 12c_4 s^{-5}/5 - (19 + 20\beta)a_3 b_3 s^{-4}. \quad \text{[A.12e]}$$

The solution of [A.8]–[A.11] has the form of [37a–d] with Σ, Σ_1 and Σ_2 expressed as follows:

$$\Sigma = -2s^2 + 3s - 3s^{-3} + 2s^{-4}, \quad \text{[A.13]}$$

$$\Sigma_1 = -2A_4 + 3A_4 s^{-1} - (A_1 - A_2 + A_3 - A_4)s^{-3} - (A_2 - 2A_1)s^{-4} \quad \text{[A.14]}$$

and

$$\Sigma_2 = 2(A_4 - A_3)s^2 + (A_1 + A_2)s - 5A_4 s^{-1} + 3(A_4 - A_3)s^{-3} + (4A_1 - A_2)s^{-4}. \quad \text{[A.15]}$$